Case Studies in Thermal Engineering 39 (2022) 102470

Contents lists available at ScienceDirect

Case Studies in Thermal Engineering

journal homepage: www.elsevier.com/locate/csite

Improvement of heat sink performance using paraffin/graphite/hydrogel phase change composite coating

Sreedevi Paramparambath [a,1], Muni Raj Maurya [a,b,1], Mohammad Talal Houkan [b], John-John Cabibihan [b], Kishor Kumar Sadasivuni [a,*]

[a] Center for Advanced Materials, Qatar University, P.O. Box. 2713, Qatar
[b] Department of Mechanical and Industrial Engineering, College of Engineering, Qatar University, P.O. Box. 2713, Qatar

HIGHLIGHTS

- Formulation of Paraffin Wax-Graphite-Hydrogel as a novel composite with enhanced properties.
- Thermal properties of composite PCM were measured and analyzed.
- The thermal conductivity of PCM composite is ~12-fold higher than paraffin.
- Low-cost, simple, and scalable technology with applicability in passive cooling.
- Effective passive cooling of solar panels by PCM composite was validated.

GRAPHICAL ABSTRACT

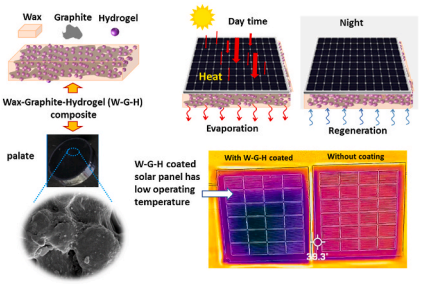

ARTICLE INFO

Keywords:
Wax-graphite-hydrogel
Composite
Thermal conductivity
Heat sink
Coating

ABSTRACT

Phase-change materials offer high latent heat and are widely used for energy storage applications. Paraffin wax is usually used as a phase-change material. However, its application in energy storage is restricted due to its low thermal conductivity. In the present work, graphite and graphite-hydrogel are used to enhance the thermal conductivity and heat release properties of paraffin wax. Wax-graphite (W-G) and wax-graphite-hydrogel (W-G-H) composites were synthesized by the dispersion of graphite and graphite-hydrogel in paraffin wax above its melting temperature. Scanning electron microscope (SEM) analysis was used to investigate the graphite and graphite-hydrogel distribution in the paraffin wax matrix. Thermogravimetric analysis (TGA) and differential scanning calorimeter (DSC) characterization were performed to measure the thermal stability and phase transition properties, respectively. DSC revealed that all composites have a similar melting temperature. The W-G-H composite displayed nearly 12 folds more thermal conductivity compared to the pure paraffin wax. High temperature brings adverse

* Corresponding author.
E-mail address: kishorkumars@qu.edu.qa (K.K. Sadasivuni).
[1] Equal contribution as the first author.

https://doi.org/10.1016/j.csite.2022.102470
Received 19 May 2022; Received in revised form 11 September 2022; Accepted 4 October 2022
Available online 6 October 2022
2214-157X/© 2022 The Authors. Published by Elsevier Ltd. This is an open access article under the CC BY license (http://creativecommons.org/licenses/by/4.0/).

impacts on energy efficiency, and even destroys a semiconductor device. The synthesized W-G-H composite is proposed to decrease the working temperature of semiconductor devices. As an applicative demonstration, the W-G-H composite film was coated at the back of the solar panel. The W-G-H composite coated solar panel displayed a surface temperature that was near ~4 °C lower than the bare solar panel while operating. The real-time experiment indicates that the W-G-H composite has high thermal conductivity and heat release properties. The study reports fundamentally new low-cost, simple, scalable, and self-adaptive, passive cooling technology to the semiconductor industry. The proposed material can further be developed in the form of paint and its heat sink properties can be improved by introducing hydrogels doped with Li^+ and Br^- ions.

Author statement

Sreedevi contributed in the Methodology, Analysis and Writing the first draft of the manuscript. Muni Raj performed Formal analysis, Validation and Final manuscript writing. Mohammad contributed in Data curation and Methodology. John-John contributed in Validation, Supervision, Writing - review & editing of the manuscript and Funding acquisition. Kishor contributed in conceptualization, supervision, Writing - review & editing and validation.

1. Introduction

Thermally conductive materials such as ceramics, polymer composites, carbon materials, and metals have gained much prominence in recent years. Polymer composites are attractive due to the features such as low density, chemical stability, and ease of processing Ref. [1]. Using thermally conductive additives, the intrinsically low thermal conductivity of the polymer composites can be enhanced. The materials that can absorb heat and release it during their phase-changing process are termed phase-changing materials (PCMs) and have gained much attraction due to their stability and high latent heat Ref. [2]. Phase-changing materials require some distinctive properties such as high heat of fusion per unit mass, high specific heat, and high latent heat storage. Compared to inorganic phase materials Ref. [3-5], organic phase change materials are less expensive, have wide melting temperatures, and show a medium range of enthalpies Ref. [2,6,7]. Paraffin wax is the organic phase material that is widely used due to its ability to melt, high storage capacity, and ability to solidify completely Ref. [8]. Besides, they are chemically inert. However, paraffin exhibits inherent low thermal conductivity and easy leakage in the liquid state. Here, for the practical application, a low thermal conductivity should be increased to improve the efficiency of thermal energy collection and release during the heating and cooling processes. Studies have been dedicated to preparing composites with enhanced thermal conductivity by infusing thermal conductive metals, fins, and carbon material in the matrix of paraffin wax Ref. [8-13]. Carbon-based materials such as graphene, carbon nanotubes, and graphite have an intrinsically high thermal conductivity which attracts the attention of researchers to improve the thermal conductivity of paraffin wax Ref. [14,2,13]. Compared to other carbon-based materials, using graphite as a thermally conductive additive considerably decreases the production cost and also have advantages such as high resistance to corrosion, good compatibility with paraffin and high stability. Graphite foams and graphite additives have been proposed to improve the thermal conductivity of the PCMs Ref. [13]. These materials have been applied as heat sink coating to decrease the working temperature of the devices. However, they suffer from the low capacity of heat dissipation and don't meet the requirements of an effective heat sink for semiconductor devices. Insufficient heat removal leads to localized overheating that, significantly impairs the device's efficiency and lifespan of devices [15]. A variety of active and passive heat dissipation approaches have been implemented to decrease the working temperature of semiconductor devices Ref. [16,17,13]. Active heat dissipation strategies needs complex accessories (e.g., water pumps and fans) that is itself consume a subsequent amount of energy and limit its application on a larger scale Ref. [18]. While, passive cooling has the advantage of no energy consumption over active cooling method but suffers from the low capacity of heat dissipation and scalability Ref. [17]. Simple, scalable, and self-adaptive cooling technology with effective heat dissipation remains a great challenge. The heat removal efficiency of thermally conducting materials such as W-G composite can be improved by infusing material that enhances heat dissipation through evaporative cooling.

Hydrogels are materials that are simple in structure and promote evaporative cooling. Hydrogels are hydrophilic crosslinked polymers found as a colloidal gel in which water is the dispersion medium Ref. [19]. The water in the hydrogel can self-adaptively re-enter and escape from hydrogel through an absorption and evaporation cycle. Based on these properties, it is intriguing to investigate the composite of paraffin wax, graphite, and hydrogel to increase heat conduction and dissipation simultaneously for application as heat sink coatings.

In the current work, we present a low-cost and simple structured passive cooling method to efficiently lower the operating temperature of high-density devices. We have studied the thermal conductivity and heat dissipation of paraffin wax, wax-graphite (W-G), and wax-graphite-hydrogel (W-G-H) composite. Simultaneously using graphite and hydrogel in wax matrix improves thermal conductivity and evaporative cooling.

2. Materials and methods

The paraffin wax used in the study has a melting temperature of ~50 °C. Graphite powder (99%) with a particle size of 7–11 μm and hydrogel was purchased from Alfa Aesar. The material properties are listed in Table 1.

For the synthesis of W-G composite, 11 g wax and 19 g graphite were mixed by stirring for 3 h at 70 °C. Similarly, 11 g wax, 12 g

graphite, and 7 g hydrogel were mixed in a beaker by stirring for 3 h at 70 °C for the synthesis of the W-G-H composite. The as-prepared composites and paraffin wax were molded in thermal conductive pallets using the hot presser, as shown in Fig. 1.

Scanning electron microscopy (SEM, Hitachi S-4800, Hitachi, Tokyo, Japan) was used to investigate the morphology samples. The thermal properties of the samples were measured by differential scanning calorimetry (DSC) and instrument was calibrated using Indium as reference sample. In DSC analysis, the reference and sample were kept at the same temperature and the thermal analysis was executed at an heating rate of 2 °C/min and temperature range from 0 to 80 °C. Thermogravimetry analysis (TGA) of samples was conducted in inert conditions with a NETZSCH STR 409C thermal analyzer at a heating rate of 2 °C/min.

3. Results and discussion

3.1. Scanning electron microscopy analysis

SEM analysis was carried out to observe the morphological changes by the dispersion of graphite and graphite-hydrogel in a pure paraffin wax matrix, as shown in Fig. 2. Fig. 2a and b shows the SEM image of wax and graphite, respectively. The surface morphology of the wax-graphite composite is presented in Fig. 2c. The graphite is well dispersed in the wax matrix without obvious aggregation, and porous structures on the surface can be noticed. Interestingly, with the addition of the hydrogel in the wax-graphite-hydrogel composite, smooth surface morphology was observed and hydrogel was well decked in the wax-graphite matrix, as shown in Fig. 2d. The addition of hydrogel has filled the pores and introduced a connected interface of particles with smooth surface morphology. This reduces the stress concentration. A direct interface among adjacent particles could improve thermal conductivity.

3.2. Thermogravimetric analysis

TGA analysis was carried out to find the thermal stability of the material and the fraction of volatile components by monitoring the weight change of the samples when heated at a temperature range of 30–800 °C. Fig. 3 shows the TGA curve, representing the percentage decomposition of hydrogel, wax, W-G, and W-G-H composite. In the case of the hydrogel, the first stage of decomposition was observed at ~240 °C, which was due to the initial decomposition of the hydrogel chain and the weight loss of residual moisture. Almost 85% of weight loss occurred at 800 °C. As expected, graphite offered high stability until 600 °C and started oxidizing when the temperature increased above 600 °C. Results indicate that the oxidations start at around 600 °C. The paraffin wax TGA analysis results suggest that the gasification started at 200 °C and it ended when the temperature reached 310 °C. In the case of the W-G composite, the first decomposition initiated at 200 °C, which corresponded to the decomposition of the wax. After that from 300 to 600 °C, the material was stable due to the presence of graphite. Above 600 °C, the gradual loss in weight was due to oxidation and burn-off of the graphite. A similar trend in weight loss was noticed for the W-G-H composite. However, above 300 °C, an almost constant difference in weight loss was observed for W-G and W-G-H composite, as shown in Fig. 2. This can be attributed to the decomposition of hydrogel in the W-G-H composite, which lowered the weight loss percentage of W-G-H compared to the W-G sample.

3.3. Differential scanning calorimeter analysis

Fig. 4 represents the DSC curves for the thermal analyses of wax, W-G, and W-G-H composite in the temperature range of 0–80 °C. Samples were placed in the DSC furnace and subjected to heating and cooling cycles. To establish the repeatability of results, samples were exposed to five successive thermal cycles. Second, heating and cooling scan cycles were considered to avoid the influence of the thermal history. The positive heat flux represents the heat absorbed during heating, and negative heat flow values while cooling indicates heat released during solidification. Fig. 4a shows the DSC plot of the pure paraffin wax having two main transition peaks and two subsidiary peaks at the left. The main peaks corresponded to the solid-liquid phase change, while the subsidiary peak represents the solid-solid transition of the wax. The estimated melting temperature of the wax is ~37 °C. The paraffin wax DSC curve agrees well with the available literature values Ref. [22-24]. Notably, both W-G and W-G-H composite exhibit thermal characteristics similar to paraffin wax as shown in Fig. 4b and c, respectively. The solid-liquid transition temperature coincides with a standard deviation of ±1 °C. It indicates that the wax in the composite transform to liquid during the solid-liquid transition and graphite, and hydrogel retain their morphology. Furthermore, it suggests no chemical reactions among wax, graphite, and hydrogel. Cycles of heating/cooling were repeated 10 times on the W-G-H composite to test the thermo-chemical stability of the composite and the repeatability of measurement. Fig. 4c shows the DSC plot of W-G-H for cycle 1 and cycle 10. The composite exhibits marginal deviation in the DSC plot. The phase-change temperatures of W-G-H composite keep constant after 10 cycles, representing the composite's stability and repeatability against thermal cycle.

3.4. Thermal conductivity studies

Fig. 5 shows the thermal conductivity studies of the wax, W-G, and W-G-H composite. Thermal conductivity measurement was

Table 1
Thermal properties of paraffin wax and graphite.

Properties	Paraffin Wax Ref. [20]	Graphite Ref. [21]
Thermal conductivity	0.2–0.24 $Wm^{-1}K^{-1}$	25-470 $Wm^{-1}K^{-1}$ (z-axis), 3000 $Wm^{-1}K^{-1}$ (in plane)
Specific heat	2.14–2.9 $Jg^{-1}K^{-1}$	0.72 $Jg^{-1}K^{-1}$
Heat of fusion	200–220 J/g	117000 J/mol
Heat storage capacity	150 kJ kg^{-1}	–

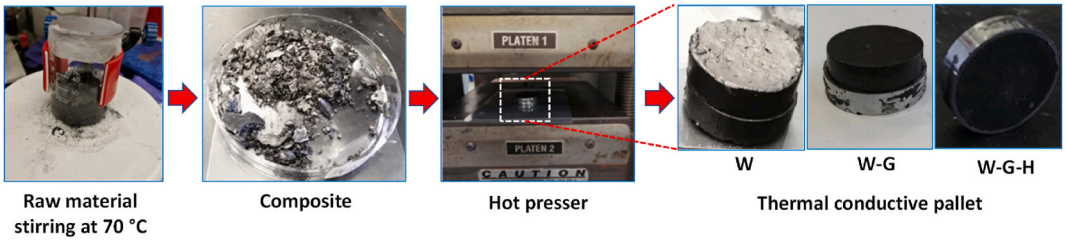

Fig. 1. Methodology for the fabrication of thermal conductive films. Step 1: mixing the raw material using a stirrer and form a composite. Step 2: Fabricating pallets of the composite materials using the hot press method.

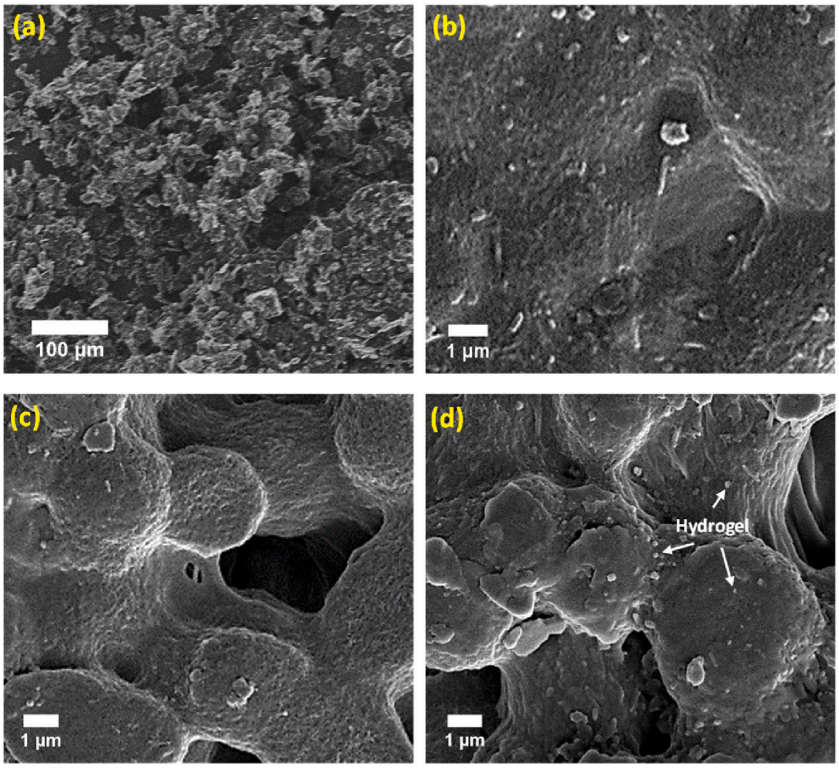

Fig. 2. SEM image of (a) Graphite powder. (b) Wax. (c) Wax-graphite. (d) Wax-graphite-hydrogel.

carried out using Fourier law. This law is applied for one-dimensional heat conduction. According to Fourier law, the equation for heat conduction is given by Equation (1).

$$Q = -\kappa A(\Delta T/\Delta x)\epsilon \quad (1)$$

In the Fourier equation, ϵ is the representation for the correction factor of heat loss and other uncertainties. ΔT represents the temperature difference between the hot and cold sides. Thermal conductivity is represented by κ with unit $Wm^{-1}K^{-1}$. The sample thickness, heat supplied, and area are represented by Δx, Q, and A, respectively. Fig. 5a and b represent the temperature distribution in the wax and W-G composite. Compared to wax and W-G composite, W-G-H composite exhibits better temperature distribution, as shown in Fig. 5c. The thermal conductivity comparison of the pure wax, W-G, and W-G-H composite is presented in Fig. 5d. The higher thermal conductivity is found for the W-G-H composite with thermal conductivity of 3.24 $Wm^{-1}K^{-1}$. The inter-chain heat efficiency of the hydrogel is enhanced by the hydrogen bond present in the hydrogel (i.e., the dynamic intermolecular forces break and constantly reform), which could lead to the enhancement in thermal transport. The thermal conductivity of W-G composite and pure paraffin wax was estimated to be 0.88 $Wm^{-1}K^{-1}$ and 0.26 $Wm^{-1}K^{-1}$, respectively. Table 2 compares the thermal conductivity of the W-G-H composite with the paraffin wax composites reported in the literature. In comparison to the other reported paraffin wax composite, the W-G-H composite exhibits high thermal conductivity. The enhanced heat transfer of the W-G-H composite can be attributed to the high degree of graphitization and efficient stacking of graphite through embedded hydrogel particles.

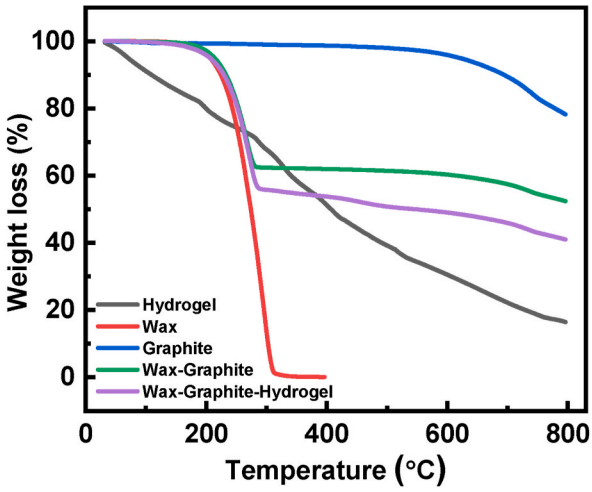

Fig. 3. TGA analysis of hydrogel, wax, graphite, wax-graphite (W–G), and wax-graphite-hydrogel (W-G-H) composite. Representing the percentage decomposition of hydrogel, wax, W-G, and W-G-H composite with respect to the increase in temperature.

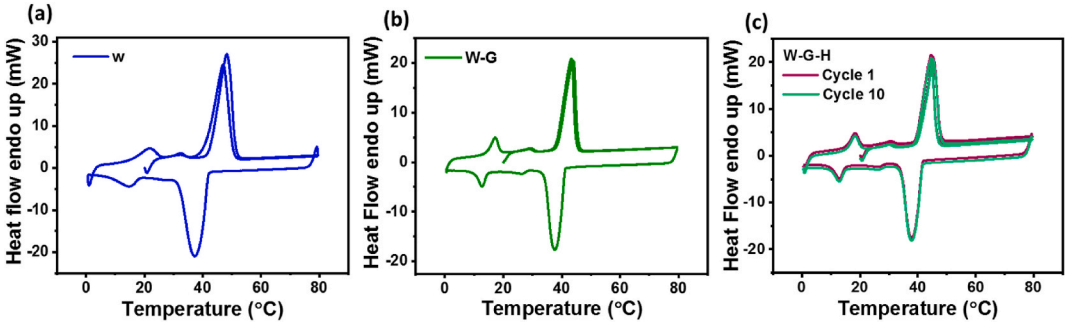

Fig. 4. DSC plot of (a) Wax. (b) Wax-graphite (W–G). (c) Wax-graphite-hydrogel (W-G-H) composite for DSC analysis cycle 1 and cycle 10. A transition peak at ~37 °C is observed for all samples, suggesting that the wax in the composite transforms to liquid during solid-liquid transition and graphite, and hydrogel retains their morphology.

3.5. Real-time thermal conductivity studies

Fig. 6 shows the influence of wax, W-G, and W-G-H composite heat conduction on melting an ice block. In the experiment, the ice block was sandwiched between the fabricated wax, W-G, and W-G-H pallet, as shown in Fig. 6a. When the pallets are placed in contact with the ice block temperature gradient is formed, and heat readily flows through the interfaces. Moreover, the rate of ice melting majorly depends on the heat conductivity of the different composite pallets. Gradual, consistent melting of ice was observed for the W-G-H composite. The wax showed the slowest ice melting rate among individual specimens and W-G-H achieved the highest melting rate. Fig. 6b shows the samples and left-over ice photographs after 60 s. It was observed that after 60 s, almost 3/4th portion of the ice melted in the case of W-G-H. Whereas W-G composite could melt nearly 1/4th of the ice and not much ice melting was noticed in the case of wax. Thus, from the above investigation, it can be inferred that the W-G-H composite exhibited high thermal conductivity compared to the W-G composite and paraffin wax.

3.6. Heat sink coating

To investigate the W-G-H composite properties as a heat sink coating, a ~1 mm thick W-G-H coating was applied at the back of the solar panel using the blade coating method. Both solar panels with and without W-G-H coating were placed adjacent to each other, and a real-time experiment was performed under clear sky conditions at 11:00 a.m. Fig. 7a shows the schematic, representing thermal conduction and solar panel surface temperature lowering through the W-G-H coating. The hydrogel in the composite absorbed the moisture from the surroundings, and the carbon derivative flakes acted as a thermal conductor that transferred the heat from the solar panel to the hydrogel. The hydrogel has taken the heat from the flakes and released the absorbed moisture back into the environment. As a result, the heat from the solar panel was utilized in releasing the water content absorbed by the hydrogel, and the solar panel temperature is lowered. Fig. 7b shows the thermal image of the solar panels, both with and without W-G-H coating. The thermal mapping indicates that the solar panel coated with a W-G-H composite (left image) exhibited a lower surface temperature than the solar panel without coating. The surface temperature of the bare solar panel was ~39.3 °C, while the W-G-H coated solar panel

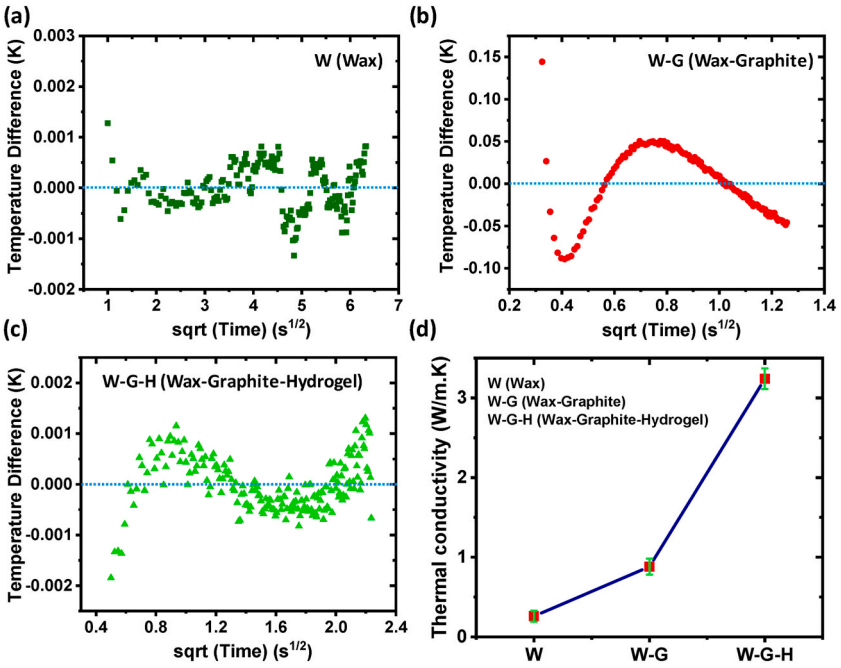

Fig. 5. Thermal conductivity studies of (a) wax, (b) wax-graphite, (c) wax-graphite-hydrogel, and (d) thermal conductivity comparison between all three composites. Compared to wax and W-G composite, W-G-H composite exhibits better temperature distribution and exhibits enhanced thermal conductivity.

Table 2
Comparison of the thermal conductivity enhancement with different fillers in paraffin wax.

PCM	κ of original PCM [W m^{-1} K^{-1}]	Additive	κ of composite PCM [W m^{-1} K^{-1}]	Reference
Paraffin wax	0.26	Graphene oxide + carbon nanotubes aerogel	0.40	Ref. [25]
Paraffin wax	0.25	Carbon foam	0.43	Ref. [26]
Paraffin wax	0.37	Cu nanowires aerogel	0.48	Ref. [27]
Paraffin wax	0.25	Carbon fibers foam	0.77 (axial)	Ref. [28]
Paraffin wax	0.27	Carbon textile	0.99	Ref. [29]
Paraffin wax	0.27	Graphene foam	1.22	Ref. [30]
Paraffin wax	0.25	Carbon fibers	1.73	Ref. [31]
Paraffin wax	0.26	Graphite + hydrogel	3.24	**Present work**

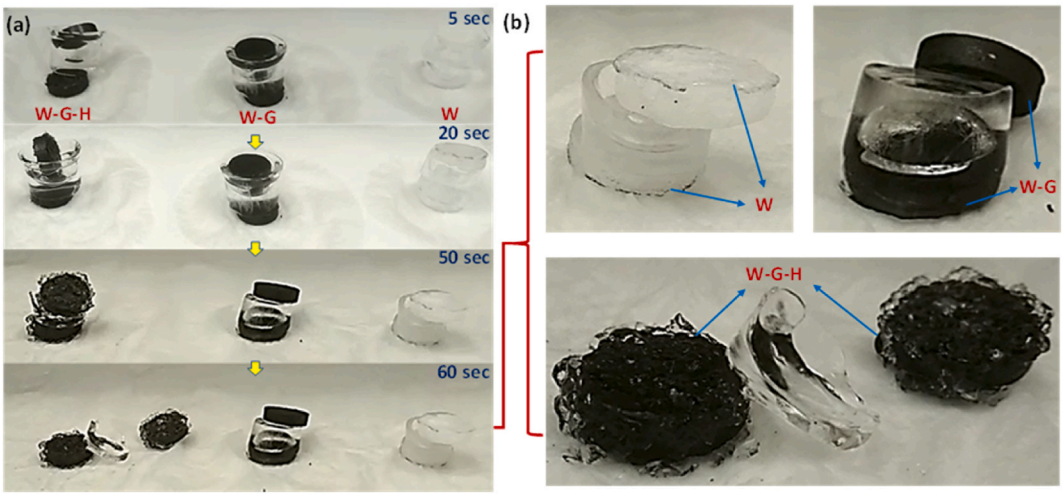

Fig. 6. Real-time experiment representing melting of ice via heat sink effect. (a) The ice was melted by wax, W-G, and W-G-H composite at different timestamps. (b) Photograph displaying samples and left-over ice after 60 s.

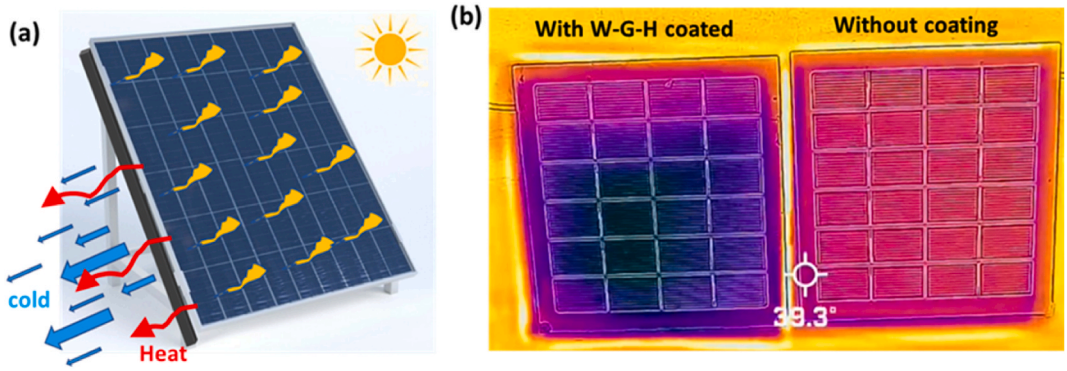

Fig. 7. Heat sink coating on a solar panel. (a) Schematic representing heat sink by W-G-H coating applied on the back of the solar panel. (b) Thermal image representing solar panel surface temperature mapping coated with W-G-H composite (left) and without coating (right).

displayed ~35 °C. The above investigation indicated that the W-G-H coating successfully lowered the solar panel surface temperature by nearly 4 °C and is best suited for temperature management of semiconductor devices.

4. Conclusions

In summary, improvement in the heat transfer property of paraffin wax was demonstrated by incorporating graphite-hydrogel in the wax matrix. The wax-graphite-hydrogel (W-G-H) composite was synthesized by simple and low-cost dispersion and melting. Furthermore, a composite pallet was fabricated by compression method. The SEM results showed that the graphite and hydrogel were well dispersed in a wax matrix with smooth surface morphology. DSC characterization revealed no significant effect on the phase change temperature of paraffin wax after the utilization of graphite and hydrogel. Thermal studies indicated that the loading of graphite and hydrogel boosted the wax heat storage and release rate. The thermal conductivity of paraffin wax was effectively improved by ~12 folds from 0.26 $Wm^{-1}K^{-1}$ to 3.24 $Wm^{-1}K^{-1}$ in the W-G-H composite. The efficient passive cooling strategy was validated by applying synthesized PCM coating at the back of the solar panel. The operating temperature of the W-G-H coated solar panel was successfully decreased by a margin of ~4 °C compared to the bare solar panel. In conclusion, this work brings low-cost, scalable, self-adaptive passive cooling technology as a universal approach for temperature management in solar and semiconductor industries.

Declaration of competing interest

The authors declare that they have no known competing financial interests or personal relationships that could have appeared to influence the work reported in this paper.

Data availability

No data was used for the research described in the article.

Acknowledgment

This work was supported by Qatar National Research Fund under the grant no. NPRP12S-0131-190030. The statements made herein are solely the responsibility of the authors. Open Access funding was provided by the Qatar National Library

References

[1] X. Xu, J. Chen, J. Zhou, B. Li, Thermal conductivity of polymers and their nanocomposites, Adv. Mater. 30 (2018), 1705544, https://doi.org/10.1002/adma.201705544.
[2] X. Zhang, R. Wen, Z. Huang, C. Tang, Y. Huang, Y. Liu, M. Fang, X. Wu, X. Min, Y. Xu, Enhancement of thermal conductivity by the introduction of carbon nanotubes as a filler in paraffin/expanded perlite form-stable phase-change materials, Energy and Buildings, Energy Build. 149 (2017) 463–470, https://doi.org/10.1016/j.enbuild.2017.05.037.
[3] N. Aslfattahi, R. Saidur, N.A. Che Sidik, M.F. Mohd Sabri, M.H. Zahir, Experimental assessment of a novel eutectic binary molten salt-based hexagonal boron nitride nanocomposite as a promising PCM with enhanced specific heat capacity, J. Adv. Res. Fluid Mech. Therm. Sci. 68 (2020) 73–85. https://akademiabaru.com/submit/index.php/arfmts/article/view/2918.
[4] Samylingam, N. Aslfattahi, K. Kadirgama, M. Samykano, L. Samylingam, R. Saidur, Improved thermophysical properties of developed ternary nitrate-based phase change material incorporated with MXene as novel nanocomposites, Energy Eng. J. Assoc. Energy Eng. 118 (2021), https://doi.org/10.32604/EE.2021.016087.
[5] I. Samylingam, K. Kadirgama, N. Aslfattahi, L. Samylingam, R. Devarajan, S. Harun, S. Mahendran, R. Saidur, Review on thermal energy storage and eutectic nitrate salt melting point, IOP Conf. Ser. Mater. Sci. Eng. 1078 (2021), 012034, https://doi.org/10.1088/1757-899X/1078/1/012034.
[6] C. Zeng, S. Liu, A. Shukla, Adaptability research on phase change materials based technologies in China, Renew. Sust. Energ. Rev. 73 (2017) 145–158, https://doi.org/10.1016/j.rser.2017.01.117.

[7] Y. Xu, A.S. Fleischer, G. Feng, Reinforcement and shape stabilization of phase-change material via graphene oxide aerogel, Carbon 114 (2017) 334–346, https://doi.org/10.1016/j.carbon.2016.11.069.
[8] P. Cheng, X. Chen, H. Gao, X. Zhang, Z. Tang, A. Li, G. Wang, Different dimensional nanoadditives for thermal conductivity enhancement of phase change materials: fundamentals and applications, Nano Energy 85 (2021), 105948.
[9] N. Aslfattahi, R. Saidur, A. Arifutzzaman, R. Sadri, N. Bimbo, M.F.M. Sabri, P.A. Maughan, L. Bouscarrat, R.J. Dawson, S.M. Said, B.T. Goh, N.A.C. Sidik, Experimental investigation of energy storage properties and thermal conductivity of a novel organic phase change material/MXene as A new class of nanocomposites, J. Energy Storage 27 (2020), 101115, https://doi.org/10.1016/j.est.2019.101115.
[10] F. Zhu, C. Zhang, X. Gong, Numerical analysis on the energy storage efficiency of phase change material embedded in finned metal foam with graded porosity, Appl. Therm. Eng. 123 (2017) 256–265, https://doi.org/10.1016/j.applthermaleng.2017.05.075.
[11] N. Aslfattahi, R. Saidur, A. Arifutzzaman, A.S. Abdelrazik, L. Samylingam, M.F.M. Sabri, N.A.C. Sidik, Improved thermo-physical properties and energy efficiency of hybrid PCM/graphene-silver nanocomposite in a hybrid CPV/thermal solar system, J. Therm. Anal. Calorim. 147 (2022) 1125–1142, https://doi.org/10.1007/s10973-020-10390-x.
[12] A. Zendehboudi, N. Aslfattahi, S. Rahman, M.F. Mohd Sabri, S. Mohd Said, A. Arifutzzaman, N.A. Che Sidik, Optimization of thermal conductivity of nano PCM-based graphene by response surface methodology, J. Adv. Res. Fluid Mech. Therm. Sci. 75 (2021) 108–125. https://akademiabaru.com/submit/index.php/arfmts/article/view/3104.
[13] S. Yeo, J. Yun, S. Kim, M.S. Cho, Y.W. Lee, Fabrication methods and anisotropic properties of graphite matrix compacts for use in HTGR, J. Nucl. Mater. 499 (2018) 383–393, https://doi.org/10.1016/j.jnucmat.2017.11.055.
[14] A.S.F. Mahamude, W.S.W. Harun, K. Kadirgama, K. Farhana, D. Ramasamy, L. Samylingam, N. Aslfattahi, Thermal performance of nanomaterial in solar collector: state-of-play for graphene, J. Energy Storage 42 (2021), 103022, https://doi.org/10.1016/j.est.2021.103022.
[15] C. Sun, Y. Zou, C. Qin, B. Zhang, X. Wu, Temperature effect of photovoltaic cells: a review, Adv. Compos. Hybrid Mater. (2022), https://doi.org/10.1007/s42114-022-00533-z.
[16] H.G. Teo, P.S. Lee, M.N.A. Hawlader, An active cooling system for photovoltaic modules, Appl. Energy 90 (2012) 309–315, https://doi.org/10.1016/j.apenergy.2011.01.017.
[17] S.K. Mohammadian, Y. Zhang, Thermal management optimization of an air-cooled Li-ion battery module using pin-fin heat sinks for hybrid electric vehicles, J. Power Sources 273 (2015) 431–439, https://doi.org/10.1016/j.jpowsour.2014.09.110.
[18] K. Górecki, K. Posobkiewicz, Cooling systems of power semiconductor devices—a review, Energies 15 (2022) 4566, https://doi.org/10.3390/en15134566.
[19] Z. Liu, W. Toh, T.Y. Ng, Advances in mechanics of soft materials: a review of large deformation behavior of hydrogels, Int. J. Appl. Mech. 7 (2015), 1530001, https://doi.org/10.1142/S1758825115300011.
[20] M. Lachheb, K. Mustapha, A. Fethi, B.N. Sassi, F. Magali, S. Patrik, Thermal properties measurement and heat storage analysis of paraffin/graphite composite phase change material, Compos. B Eng. 66 (2014) 518–525, https://doi.org/10.1016/j.compositesb.2014.05.011.
[21] R. Sengupta, M. Bhattacharya, S. Bandyopadhyay, A.K. Bhowmick, A review on the mechanical and electrical properties of graphite and modified graphite reinforced polymer composites, Prog. Polym. Sci. 36 (2011) 638–670, https://doi.org/10.1016/j.progpolymsci.2010.11.003.
[22] R.S. Kumar, D.J. Krishna, Differential Scanning Calorimetry (DSC) analysis of latent heat storage materials for low temperature (40–80 °C) solar heating applications, Int. J. Eng. Res. Technol. 2 (2013) 429–455.
[23] H. Ettouney, I. Alatiqi, M. Al-Sahali, K. Al-Hajirie, Heat transfer enhancement in energy storage in spherical capsules filled with paraffin wax and metal beads, Energy Convers. Manag. 47 (2006) 211–228.
[24] M.A. Mahmud, S. Kamaruzzaman, M. Sohif, Fabrication and experimental investigation of PCM capsules integrated in solar air heater, Am. J. Environ. Sci. 7 (2011) 542, https://doi.org/10.3844/ajessp.2011.542.546.
[25] G. Chen, Y. Su, D. Jiang, L. Pan, S. Li, An experimental and numerical investigation on a paraffin wax/graphene oxide/carbon nanotubes composite material for solar thermal storage applications, Appl. Energy 264 (2020), 114786, https://doi.org/10.1016/j.apenergy.2020.114786.
[26] N. Sheng, T. Nomura, C. Zhu, H. Habazaki, T. Akiyama, Cotton-derived carbon sponge as support for form-stabilized composite phase change materials with enhanced thermal conductivity, Sol. Energy Mater. Sol. Cells 192 (2019) 8–15, https://doi.org/10.1016/j.solmat.2018.12.018.
[27] L. Zhang, L. An, Y. Wang, A. Lee, Y. Schuman, A. Ural, A.S. Fleischer, G. Feng, Thermal enhancement and shape stabilization of a phase-change energy-storage material via copper nanowire aerogel, Chem. Eng. J. 373 (2019) 857–869, https://doi.org/10.1016/j.cej.2019.05.104.
[28] N. Sheng, R. Zhu, K. Dong, T. Nomura, C. Zhu, Y. Aoki, H. Habazaki, T. Akiyama, Vertically aligned carbon fibers as supporting scaffolds for phase change composites with anisotropic thermal conductivity and good shape stability, J. Mater. Chem. 7 (2019) 4934–4940, https://doi.org/10.1039/C8TA11329G.
[29] N. Sheng, Z. Rao, C. Zhu, H. Habazaki, Enhanced thermal performance of phase change material stabilized with textile-structured carbon scaffolds, Sol. Energy Mater. Sol. Cells 205 (2020), 110241, https://doi.org/10.1016/j.solmat.2019.110241.
[30] G. Qi, J. Yang, R. Bao, D. Xia, M. Cao, W. Yang, M. Yang, D. Wei, Hierarchical graphene foam-based phase change materials with enhanced thermal conductivity and shape stability for efficient solar-to-thermal energy conversion and storage, Nano Res. 10 (2016) 802–813, https://doi.org/10.1007/s12274-016-1333-1.
[31] N. Sheng, Z. Rao, C. Zhu, H. Habazaki, Honeycomb carbon fibers strengthened composite phase change materials for superior thermal energy storage, Appl. Therm. Eng. 164 (2020), 114493, https://doi.org/10.1016/j.applthermaleng.2019.114493.